Optical response of conjugated polyenes.
Electrons, holes and intermediate excitons

Hong Xiang Wang and Shaul Mukamel

Department of Chemistry, University of Rochester, Rochester, NY 14627, USA

A real-space representation of the optical response of conjugated polyenes is developed by starting with the Pariser–Parr–Pople Hamiltonian, and using the Wannier representation to derive equations of motion for coupled two-site oscillators representing correlated electron–hole pairs. The resulting elementary excitations are shown to be intermediate between the molecular (Frenkel) and the semiconductor (Wannier) excitons, and clearly resemble charge-transfer excitons. The present approach allows a unified treatment of the optical response of molecular and semiconductor materials.

1. Introduction

The optical response of π-conjugated or σ-conjugated molecules is of considerable current interest [1–3]. Extensive effort has been made towards measuring the linear and the nonlinear optical response of amorphous or crystalline conjugated polymers. Techniques employed include linear absorption, fluorescence, reflection, second harmonic generation (SHG), third harmonic generation (THG), two-photon absorption (TPA), and pump–probe spectroscopy [4–7]. Linear polyenes belong to the C_{2h} symmetry group, and the ground state has an A_g symmetry. The allowed one-photon transitions are, therefore, to excited states with B_u symmetry, and the final state in two-photon absorption must have the same symmetry as the ground state. Two important observations were made in the studies of the electronic structure of small conjugated molecules. The first is the change of the relative energy of the $2\,^1A_g$ and $1\,^1B_u$ states. It has been shown that when the electron–electron interactions are incorporated, the $2\,^1A_g$ state is below the $1\,^1B_u$ state, whereas in the one-electron model the order is reversed. In addition, it has been shown that only a few "essential states" make the dominant contribution to the optical response of short polyenes [1,4,8–10]. Figuring out the nature of these few essential states for large polyenes constitutes a major open challenge in understanding the origin of the optical response of conjugated molecules. An extensive theoretical effort is currently directed towards the calculation and the interpretation of these linear and nonlinear optical measurements [1–3,10–14]. Both ab initio and semi-empirical calculations were employed in the attempt to identify the essential states, and predict their relative positions.

The conventional molecular methods evaluate the optical response using summations over molecular states, which require the calculation of the transition energies and the transition dipole matrix elements among all the molecular states. These calculations, though remarkably accurate, are very tedious and are therefore limited to relatively small systems such as octatetraene [1]. Moreover, the lack of a good single-particle basis set makes it difficult to establish a simple physical picture of the optical response, even for systems where these calculations can be carried out.

Alternatively, conjugated polyenes can be viewed as one-dimensional semiconductors and can be treated using many body Green function techniques [15–18], which focus on the elementary excitations (electron–hole pairs) rather than the individual molecular eigenstates. In molecular crystals (with no conjugation), the pairs created by optical excitation are localized on the same molecule and form Frenkel excitons. In semiconductors they form less tightly

bound states, which extend over many unit cells, and may show up as a Rydberg hydrogen-like progression in the optical spectrum. These are denoted Wannier excitons [15,16]. In molecular crystals there are also intermediate "charge-transfer" excitons in which the electron and the hole are separated by only one or two unit cells [19].

The main goal of this Letter is to develop an efficient and simple method for calculating the optical response of conjugated polyenes by formulating the problem using a semiconductor electron–hole picture. The approach has many advantages. It provides a clear physical picture of the optical processes, including the effects of the molecular structure, electron–electron and electron–hole interactions, and excitonic response. Phonon effects can also be readily incorporated in this picture [16–18,20]. In addition, the method can be easily applied to large systems since it actually becomes simpler as size increases (in contrast with the molecular methods where the computation effort increases drastically with size).

We have recently developed an oscillator picture for the optical response of nanostructures and applied it to molecular assemblies with Frenkel excitons [20] and to semiconductor particles (quantum dots) [16–18]. Using these equations, the effects of the exciton coherence-sizes, related to the electron–hole relative motion and to their center of mass motion were clearly analyzed. In this Letter, we shall extend these ideas to the linear optical response of conjugated polyenes, and show that it can be adequately described in terms of charge-transfer (intermediate) excitons. Instead of sum over all the molecular states, we map the optical properties onto harmonic oscillators. In our approach the few "essential oscillators" appear naturally, the charge–charge Coulomb and exchange interactions are included explicitly, and the effects of on-site and intersite interactions are also analyzed. The present theory provides a unified treatment of molecular, semiconductor and intermediate systems and can be directly extended to nonlinear optics by a systematic incorporation of anharmonicities [16–18,20]. It may therefore allow a comparison of the optical response of various types of materials, which is the subject of an ongoing lively debate [21]. The remainder of the Letter is divided as follows: in section 2, we present

the model Hamiltonian and recast it in an electron–hole form using a basis set of localized (Wannier) states. In section 3, we derive the equations of motion and develop an oscillator picture for the linear optical response. Finally, in section 4, we present numerical calculations and analysis of our results.

2. Model Hamiltonian in the Wannier representation

Virtually all theoretical modelling of conjugated polyenes focuses explicitly only on the π electrons. The σ electrons are considered in a mean field way via a periodic effective potential. The Hückel model provides a simple single-particle tight binding model in which we consider a chain of carbon atoms with a single $2p_z$ orbital on each atom. The Hückel model Hamiltonian is

$$H_0 = \sum_n |n\rangle \beta(1-\delta)\langle n+1|$$
$$+ |n\rangle \beta(1+\delta)\langle n-1| , \qquad (1)$$

where $|n\rangle$ represent an electron in the $2p_z$ orbital at the nth carbon atom. The two parameters $\beta(1-\delta)$ and $\beta(1+\delta)$ represent the alternate couplings of π electrons along the molecular chain. The SSH model commonly used for polyacetylenes adds phonon coupling to the Hückel model [12]. In this Letter, we adopt the Pariser–Parr–Pople (PPP) Hamiltonian which consists of the Hückel Hamiltonian plus the Coulomb interactions between the π electrons. In order to present the PPP Hamiltonian, and recast it in an electron–hole language, let us start with the solution of the eigenvalue problem $H_0\Phi = E\Phi$ for the Hückel model. We consider a cyclic polyene with N double bonds, and solve the Hückel Hamiltonian using periodic boundary conditions. The N lower (higher) eigenstates Φ_{vk} (Φ_{ck}) constitute of the valence (conduction) band, with energies ϵ_{vk} (ϵ_{ck}), respectively. They are given by,

$$\Phi_{vk}(x) = \frac{1}{\sqrt{2N}} \sum_{m=1}^{N} \exp(ikm)$$
$$\times \{\phi_2^{\pi}(x) \exp[if(k)] \pm \phi_1^{\pi}(x)\} , \qquad (2)$$
$$\epsilon_{vk} = \pm \beta[2(1+\delta^2) + (1-\delta^2)\cos k]^{1/2} , \qquad (3)$$

$$\tan[\tfrac{1}{2}f(k)] = \frac{(1-\delta)\sin k}{(1+\delta)+(1-\delta)\cos k}, \qquad (4)$$

$$k = 2\pi j/N; \quad j = 1, 2, ..., N. \qquad (5)$$

The $+$ and $-$ signs in eqs. (2) and (3) stand for $\nu = c$ (conduction band) and $\nu = v$ (valence band), respectively. $\phi_2^n(x) \equiv \langle x|2n\rangle$ and $\phi_1^n(x) \equiv \langle x|2n-1\rangle$ are the atomic $2p_z$ functions localized at the right-hand and left-hand side of the nth double bond. For clarity we have imposed periodic boundary conditions in the calculation of these eigenstates,

$$\Phi_{\nu k}(N+1) = \Phi_{\nu k}(1). \qquad (6)$$

Our model thus represents cyclic (circular) polyenes. This assumption of translational invariance is expected to hold better as the polyene size is increased, since the relative importance of the boundary decreases. It simplifies the following discussion, since it allows us to decouple the translation and the relative motions of the electron–hole pair. In the ground (vacuum) state of the Hückel model, all the N valence-band states Φ_{vk} are occupied by two electrons. Upon optical excitation, and electron moves from the ground state to any of the unoccupied states in the conduction band, creating a hole in the valence band. The lowest transition energy will be from the top of the valence band (HOMO) to the bottom of the conduction band (LUMO). This picture changes when the electron–hole Coulomb interactions are incorporated in the PPP Hamiltonian. The electron at site n and the hole at site m may form an exciton due to their attractive Coulomb interaction. The exciton is described by two coordinates: the overall translation of the electron–hole pair along the molecular chain, and their relative motion. The excitons are created coherently, but their motions and interactions may destroy the coherence. Their coherence sizes associated with both types of motion, control the optical response of the system [20].

In order to model the exciton formation and consider the coherence size effects, it is natural to adopt a real-space basis set. Starting with the N Bloch states $\Phi_{\nu k}(x)$, we therefore construct the following Wannier functions:

$$W_{\nu,n}(x) = \frac{1}{\sqrt{N}} \sum_k \exp(ikn)\,\Phi_{\nu k}(x),$$

$$n = 1, ..., N, \quad \nu = c, v. \qquad (7)$$

The Wannier functions form a real orthonormal basis of localized states. $W_{v,n}$ and $W_{c,n}$ are a valence band and a conduction band basis function localized at the nth double bond. Using this basis set, we now proceed in developing the semiconductor picture by introducing creation and annihilation operators for electrons and holes $c_n^\dagger$ creates an electron in the state $W_{c,n}$ and $d_n^\dagger$ creates a hole in the state $W_{v,n}$ ($n = 1, 2, ..., N$). These operators obey the Fermi commutation rules

$$[c_n, c_m^\dagger] = \delta_{nm} - 2c_m^\dagger c_n,$$

$$[d_n, d_m^\dagger] = \delta_{nm} - 2d_m^\dagger d_n. \qquad (8)$$

All other commutators ($[c_n, d_m]$ etc.) not given in eq. (8) vanish. Adopting the Wannier functions basis set, and the electron–hole representation, the PPP Hamiltonian [1] for a polyene with N double bonds and $2N$ π electrons, interacting with a classical external electric field $E(t)$, reads

$$H = \sum_{nm} [\omega_{nm}^c c_n^\dagger c_m - \omega_{nm}^v d_m^\dagger d_n + \tfrac{1}{2}V_1(nm)$$

$$\times (c_n^\dagger c_m^\dagger c_m c_n + d_n^\dagger d_m^\dagger d_n d_m - 2c_n^\dagger c_n d_m^\dagger d_m)$$

$$+ V_2(nm) c_m^\dagger c_n d_n^\dagger d_m] - PE(t). \qquad (9)$$

Here $V_1(nm)$ ($V_2(nm)$) is the Coulomb (exchange) interaction between two charges in two Wannier states at sites n and m. P is the polarization operator

$$P = \sum_{nm} (\mu_{nm}^{vc} c_n^\dagger d_m^\dagger + \mu_{mn}^{cv} d_m c_n). \qquad (10)$$

Strictly speaking, the molecular polarization P should contain also intraband transitions [18]. These transitions were neglected here since they do not affect the linear optical response and are only relevant for nonlinear optics. The electric field is $E(t) = E_0 \cos \omega t$. ω_{nm}^c (ω_{nm}^v) are the electron (hole) site energy (when $n = m$), and hopping energy (when $n \neq m$),

$$\hbar\omega_{nm}^c \equiv H_{nm}^c + \delta_{nm} \sum_{n'} [V_1(n'n) - V_2(nn)], \qquad (11)$$

$$\hbar\omega_{nm}^v \equiv H_{nm}^v + \delta_{nm} \sum_{n'} [V_1(nn) - V_1(n'n)], \qquad (12)$$

H_{nm}^c (H_{nm}^v) are the matrix elements of the Hückel Hamiltonian between two Wannier functions at site n and m in the conduction band ($+$) (valence band ($-$))

$$H^v_{nm} = \pm \frac{\beta\sqrt{2}}{N} \sum_k \exp[-ik(n-m)]\, \epsilon_{vk} . \tag{13}$$

The Hückel Hamiltonian with periodic boundary conditions is thus given by

$$H_0 = \sum_{nm} [H^c_{nm} c^\dagger_n c_m - H^v_{nm} d^\dagger_m d_n] . \tag{14}$$

μ^{cv}_{nm} is the interband transition dipole,

$$\mu^{cv}_{nm} \equiv Q \int W^*_{c,n}(x) x W_{v,m}(x)\, dx , \tag{15}$$

Q being the electron charge. These interactions may be expressed in terms of the matrix element,

$$V(^{n_1 n_2 n_3 n_4}_{\nu_1 \nu_2 \nu_3 \nu_4}) \equiv \int\int W^*_{\nu_1,n_1}(x) W^*_{\nu_2,n_2}(x') Z(x-x')$$

$$\times W^*_{\nu_3,n_3}(x') W^*_{\nu_4,n_4}(x)\, dx'\, dx , \tag{16}$$

where ν_j is the band index and n_j denote the location of the Wannier functions. $Z(x-x')$ is Ohno's expression for the Coulomb interaction

$$Z(x-x') = U[1+(x-x')^2/Q^4 U^2]^{-1/2} , \tag{17}$$

U being the on-site Hubbard interaction energy [1]. When the overlap of the Wannier functions is neglected, we get $n_1 = n_2$, and $n_3 = n_4$, and we have,

$$V_1(nm) = V(^{nmmn}_{vvvv}) = V(^{nmmn}_{cvvc})$$

$$= V(^{nmmn}_{vccv}) = V(^{nmmn}_{cccc}) , \tag{18}$$

$$V_2(nm) = V(^{nmmn}_{cvcv}) = V(^{nmmn}_{vcvc}) . \tag{19}$$

Using the translational symmetry of the system it follows that $V_1(nm)$, $V_2(nm)$, ω^v_{nm}, ω^c_{nm}, and μ^{cv}_{nm} depend only on the separation $n-m$ of the two sites.

3. Equations of motion: the exciton-oscillator picture

As indicated earlier, the motion of excitons requires considering both their relative and translational coordinates. With the present use of periodic boundary conditions, the system is translationally invariant and the center of mass motion can be easily accounted for, by changing to momentum (k) space. To that end, starting with the definition for the polarization operators (10), we change to rela-

tive coordinates $s \equiv n-m$ and the translational coordinates, $r \equiv \frac{1}{2}(n+m)$, and define

$$Y_{s,k} \equiv \frac{1}{\sqrt{N}} \sum_{r=1}^N \exp(-ikr)\, d_{r+s/2} c_{r-s/2} , \tag{20}$$

$$Y^\dagger_{s,k} \equiv \frac{1}{\sqrt{N}} \sum_{r=1}^N \exp(ikr)\, c^\dagger_{r-s/2} d^\dagger_{r+s/2} . \tag{21}$$

The linear polarization operator can then be written as

$$P^{(1)}(t) = \sum_{s,k} [\mu(s) Y^{(1)}_{s,k}(t) + \mu(s) Y^{(1)\dagger}_{s,k}(t)] . \tag{22}$$

The equation of motion for $Y_{s,k}$ is derived from the Heisenberg equation

$$\dot{Y}_{s,k} = \frac{i}{\hbar} [H, Y_{s,k}] .$$

Using the Hamiltonian (9) and the commutation relations (8), we then get

$$-i\hbar \dot{Y}^{(1)}_{s,k} = -\sum_{s'} \{\omega^v(s'-s) \exp[-ik(s'-s)]$$

$$-\omega^v(s'-s) \exp[ik(s'-s)] + V_2(s)\delta_{s'+s}$$

$$-V_1(s)\delta_{s'-s}\} Y^{(1)}_{s',k} + \mu(s)E(t)\delta_{k,0} , \tag{23}$$

where $V_1(s)$, $V_2(s)$, $\omega^v(s)$, $\mu(s)$ are given in (11)–(19) by substituting $s = n-m$, and $\mu(s) \equiv \mu^{cv}_s$, $\omega^v(s) \equiv \omega^v_s$. The equation for $Y^\dagger_{s,k}$ is obtained by a Hermitian conjugation of eq. (23).

The solution of eq. (23) can be expressed in terms of the electron–hole Green function [22]

$$G^{-1}_{s,s'}(k, \omega) \equiv \omega^c(s'-s) \exp[-ik(s'-s)]$$

$$-\omega^v(s'-s) \exp[ik(s'-s)] + V_2(s)\delta_{s'+s}$$

$$-[V_1(s)-\omega]\delta_{s'-s} . \tag{24}$$

The linear susceptibility is then given by,

$$\chi^{(1)}(\omega) = \sum_{s,s'=1}^N \mu(s)\mu(s')$$

$$\times [G_{s,s'}(k=0, \omega) + G_{s,s'}(k=0, -\omega)] . \tag{25}$$

The electron–hole Green function $G_{s,s'}(k=0, \omega)$ describes the motion of a single electron–hole pair. The Green function (and the linear susceptibility) are written here in the coordinate (real-space) representation, which provides a clear physical insight. The resulting electron–hole picture also has impor-

tant computational advantages, as will be illustrated below. For the sake of completeness let us connect this result to the more conventional sum over states expression. To that end we note that eq. (24) define an eigenvalue problem with eigenstates $\Psi_\alpha(k, x)$ and eigenvalues $E_\alpha(k)$. Using these exciton eigenstates, the Green function can be recast in the form

$$G_{s,s'}(k, \omega) = \sum_{\alpha=1}^{N} \frac{\psi_\alpha(k, s)\psi_\alpha^*(k, s')}{\omega - E_\alpha(k) + i\Gamma_\alpha} . \qquad (26)$$

Upon the substitution of eq. (26) into (25), the linear susceptibility assumes the conventional form,

$$\chi^{(1)}(\omega) = 2 \sum_{\alpha=1}^{N} \frac{E_\alpha(k=0)|\mu_\alpha|^2}{\omega^2 - E_\alpha^2(k=0) + i\omega\Gamma_\alpha} , \qquad (27)$$

where $\mu_\alpha \equiv \sum_s \psi_\alpha(k=0, s) \mu(s)$, and Γ_α is the damping rate of the α eigenstate. Eq. (27) is the familiar sum over state expression of the linear susceptibility.

4. Calculations and discussion

We start our numerical study by considering the dependence of the various coupling parameters which specify the Hamiltonian (eq. (9)) on the separation s. In all the calculations presented below we have used the interaction parameters [1] $\beta = -2.4$ eV and $U = 11.23$ eV. In fig. 1 we display the electron $\omega^c(s)$ and the hole $\omega^v(s)$ coupling, the Coulomb interaction $V_1(s)$, and the exchange interaction $V_2(s)$, for a large polyene with $N = 50$. All calculations were made using typical parameters [1] for polyacetylenes ($\delta = 0.07$), polydiacetylenes ($\delta = 0.15$), and polysilanes ($\delta = 0.33$). Figs. 1a and 1b clearly show that the hole and the electron have a different effective mass. From figs. 1c and 1d, we note that the exchange interaction is shorter range compared with the Coulomb–Coulomb interaction, which implies that the exchange interaction plays an important role for oscillators with small electron–hole separation s. As s increases, the Coulomb interactions dominate the optical response. In fig. 2 we display the variation of the interband transition dipole $\mu(s)$ with electron–hole separation s, for different values of system size and δ. $\mu(s)$ is calculated using eqs. (2), (7) and (15) by setting $s = n - m$. The following assumption was further made in the calculation of $\mu(s)$ [23]
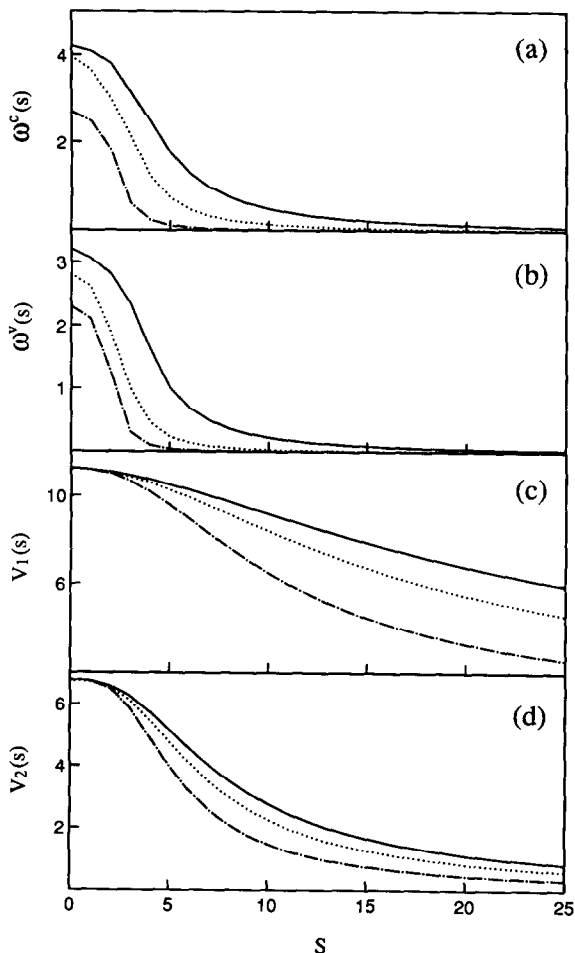

Fig. 1. Variation of the Hamiltonian coupling parameters with separation s. $N = 50$, all quantities are given in units of electron volts. Solid line: $\delta = 0.07$ (polyacetylene); dotted $\delta = 0.15$ (polydiacetylene); dot-dashed $\delta = 0.33$ (polysilane). (a) $\omega^c(s)$ conduction band coupling; (b) $\omega^v(s)$ valence band coupling; (c) $V_1(s)$ Coulomb coupling; (d) $V_2(s)$ exchange coupling.

$$\langle \phi_i^m | x | \phi_j^n \rangle = x_i^n \delta_{ij} \delta_{nm} , \qquad (28)$$

where x_i^n is the coordinate of the left side ($i = 1$) or right side ($i = 2$) of the nth double bond. Fig. 2 shows that the electron–hole pair is mainly created on the same unit cell or between nearest neighbors. For example, taking $N = 50$ and $\delta = 0.07$, we have $\mu(0) : \mu(1) : \mu(2) = 1 : 0.75 : 1.7 \times 10^{-2}$. After the creation of the pair, the electron and the hole may move apart, and their motion is determined by the electron–hole Green function. The Green function
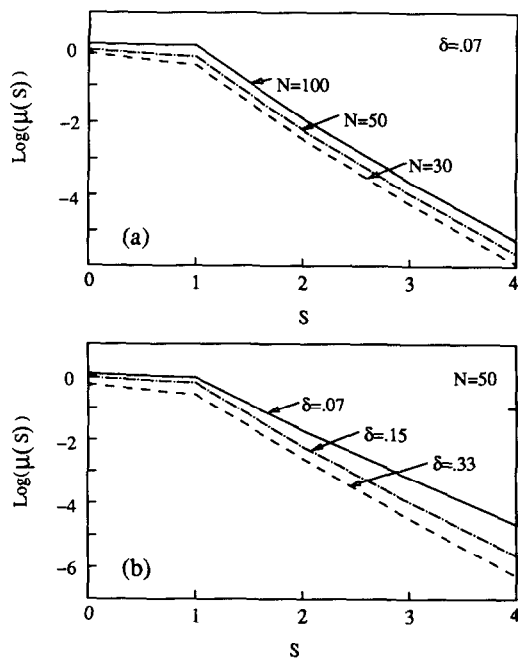
Fig. 2. (a) Interband transition dipoles $\mu(s)$ of polyacetylene for different molecular sizes. (b) $\mu(s)$ for polyacetylene, polydiacetylene, and polysilane ($\delta=0.07$, $\delta=0.15$, $\delta=0.33$) with $N=50$. All curves are in arbitrary units.
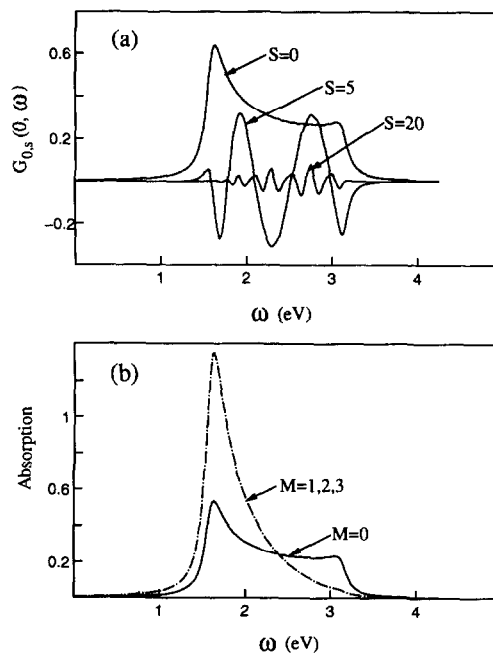

Fig. 3. (a) Green functions $G_{0,s}(0, \omega)$ with ω for polyacetylene with $N=50$ for different values of s. (b) The absorption spectrum $\mathrm{Im}[\chi_M^{(1)}(\omega)]$ for polyacetylene with $N=50$. Solid line $M=0$, dotted dash $M=1, 2, 3$.

$G_{0,s}(k=0, \omega)$ for polyacetylene with 50 double bonds, is plotted in fig. 3a as a function of ω for different values of s (0, 5, and 20). The linear optical response of the conjugated polyenes is determined by the product of $\mu(s)\mu(s')G_{s,s'}$, as shown in eqs. (25) and (27). In order to illustrate the contribution of various electron–hole separations to $\chi^{(1)}$, we have defined $\chi_M^{(1)}(\omega)$ by eq. (25) with the s, s' summation truncated as $s, s'=0, 1, ...M$. $\chi_M^{(1)}(\omega)$ for polyacetylene having 50 double bonds is plotted in fig. 3b, for $M=0, 1, 2, 3$. It shows the finite size of the exciton and the few essential oscillators. The calculation rapidly converges at $M=1$, which shows that the elementary excitations of the systems are charge-transfer excitons. Fig. 3b further illustrates the usefulness of the electron–hole representation, since the summation over eigenstates involves many terms whereas in s space we need consider only a few terms. The absorption spectra $\mathrm{Im}\chi^{(1)}(\omega)$ for both the Hückel and the PPP models were calculated for polyacetylene with 4, 10, 20, 30, 50, and 100 double bonds (N), and are displayed in fig. 4. The Hückel

calculations were made by assuming periodic boundary conditions (eq. (14)). For small molecular sizes ($N=4$), all the transitions have roughly the same intensity within the Hückel model. As N increases, the intensity of the absorption builds up at the band edge. In the PPP model, the band edge transitions always have the largest intensity. From the absorption spectrum, the band-gap is deduced and plotted in fig. 5. The band-gap in the PPP model using the parameters listed earlier in this section with periodic boundary conditions is in good agreement with Kohler's recent calculation which, in turn, provides a good fit to the experiment [4]. For comparison, the dashed line is the result for Hückel model obtained by a numerical diagonalization of eq. (1) without imposing any boundary conditions. The band-gap and the absorption intensities strongly depend on the Coulomb interactions.

In conclusion we note that the present approach is particularly suitable for calculating the nonlinear optical response of conjugated polyenes, and analyzing the role of the exciton coherence length associated
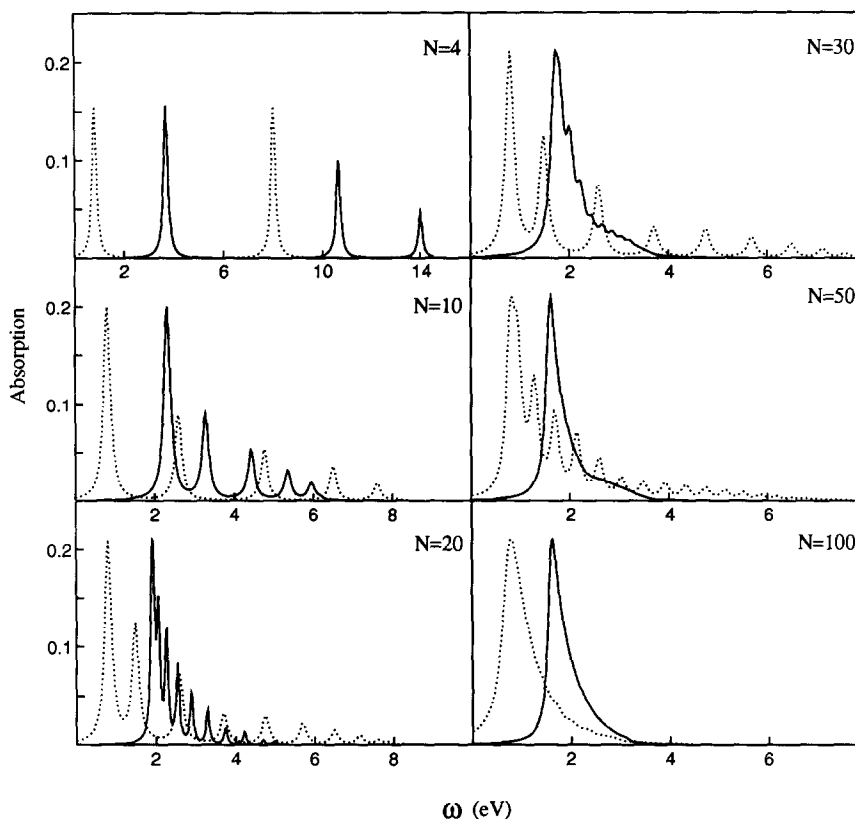
Fig. 4. The absorption spectrum $\text{Im}[\chi^{(1)}(\omega)]$ for polyacetylene with different molecular sizes. The solid line is the present electron–hole calculation using the PPP model, dotted line shows calculation for the free electron (Hückel) model with periodic boundary conditions (eq. (14)).
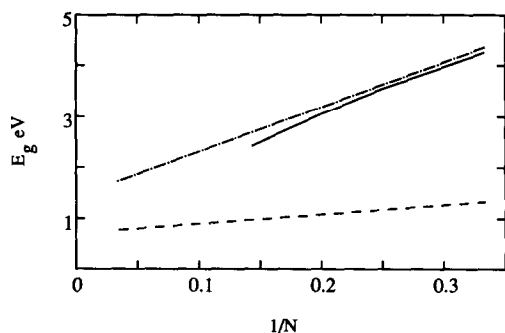

Fig. 5. The band-gap for polyacetylenes ($\delta = 0.07$) versus molecular size. Solid line is Kohler's calculation [4], dotted-dash line presents electron–hole calculation using the PPP model with periodic boundary conditions, dashed line was obtained by a numerical diagonalization of the Hückel Hamiltonian (eq. (1)) without assuming periodic boundary conditions. When periodic boundary conditions are imposed on the Hückel model, the band-gap (eq. (3)) is $4\beta\delta$, independent on size N.

with the center of mass and the relative motion of the electron and the hole [17]. This extension will be presented in the future.

Acknowledgement

References

[1] S. Etemad and Z.G. Soos, in: Spectroscopy of advanced materials, eds. R.J.H. Clark and R.E. Hester (Wiley, New York, 1991);

Z.G. Soos and S. Ramasheba, J. Chem. Phys. 90 (1988) 1067.

[2] D.J. Williams, ed., Nonlinear optical properties of organic and polyatomic materials, ACS Symp. Ser. Vol. 233 (American Chemical Society, Washington, 1985).

[3] D.S. Chemla and J. Zyss, eds., Nonlinear optical properties of organic molecules and crystals, Vols. 1, 2 (Academic Press, New York, 1987).

[4] B.S. Hudson, B.E. Kohler and K. Schulten, Excited States 6 (1982) 1;
B.E. Kohler, J. Chem. Phys. 88 (1988) 2788; 93 (1990) 5838.

[5] T. Kurihara, N. Oba, Y. Mori, S. Tomaru and T. Kaino, J. Appl. Phys. 70 (1991) 1;
S.A. Jenekhe, M.F. Roberts, A.K. Agrawal, J.S. Meth and H. Vanherzeele, Mater. Res. Soc. Symp. Proc. 214 (1991) 55;
W.E. Torruellas, D. Neher, R. Zanoni, G.I. Stegeman and F. Kajzar, Chem. Phys. Letters 175 (1990) 11.

[6] W.-S. Fann, S. Benson, J.M. Madey, S. Etemad, G.L. Baker and F. Kajdar, Phys. Rev. Letters 62 (1989) 1492;
P.D. Townsend, W.-S. Fann, S. Etemad, G.L. Baker, Z.G. Soos and P.C.M. McWilliams, Chem. Phys. Letters 180 (1991) 485.

[7] G.J. Blanchard, J.P. Heritage, A.C. Von Lehmen, M.K. Kelly, G.L. Baker and S. Etemad, Phys. Rev. Letters 63 (1989) 887;
B.I. Greene, J.F. Mueller, J. Orenstein, D.H. Rapkine, S. Schmitt-Rink and M. Thakur, Phys. Rev. Letters 61 (1988) 325;
B.C. Hess, G.S. Kanner, Z.V. Vardeny and G.L. Baker, Phys. Rev. Letters 66 (1991) 2364.

[8] K. Schulten, I. Ohmine and M. Karplus, J. Chem. Phys. 64 (1976) 4422;
I. Ohmine and M. Karplus, J. Chem. Phys. 68 (1978) 2298.

[9] A.F. Garito and J.R. Heflin, F.Y. Wong and Q. Zamani-Khamiri, in: Organic materials for nonlinear optics, eds. R.A. Teann and D. Bloor, Special Publication No. 69 (Royal Society of Chemistry, London, 1988).

[10] S.N. Dixit, D.D. Guo and S. Mazumdar, Mol. Cryst. Liquid Cryst. 194 (1991) 33;
S. Mazumdar and S.N. Dixit, Synth. Metals 28 (1989) D463;

S. Mazumdar and D.K. Campbell, Phys. Rev. Letters 55 (1985) 2067.

[11] S. Abe and W.P. Su, Mol. Cryst. Liquid Cryst. 194 (1991) 357.
J. Yu. Friedman, P.R. Baldwin and W.P. Su, Phys. Rev. B 39 (1989) 814.

[12] W.P. Su, J.R. Schrieffer and A.J. Heeger, Phys. Rev. B 22 (1980) 2099.

[13] G.P. Agrawal, C. Cojan and C. Flytzanis, Phys. Rev. B 17 (1978) 776;
C. Wu and X. Sun, Phys. Rev. B 42 (1990) 9736;
W. Wu, Phys. Rev. Letters 62 (1988) 1119.

[14] C.P. DeMelo and R. Silbey, J. Chem. Phys. 88 (1987) 2558;
C.P. DeMelo and R. Silbey, J. Chem. Phys. 88 (1987) 2587;
H.E. Schaffer, R.R. Chance, R.J. Silbey, K. Knoll and R.R. Schrock, J. Chem. Phys. 94 (1991) 4146.

[15] S. Schmitt-Rink, D.A.B. Miller and D.S. Chemla, Phys. Rev. B 35 (1987) 8113;
H. Haug and S.W. Koch, Quantum theory of the optical and electronic properties of semiconductors (World Scientific, Singapore, 1990).

[16] J.R. Kuklinski and S. Mukamel, Phys. Rev. B 42 (1990) 295.

[17] J.R. Kuklinski and S. Mukamel, Chem. Phys. Letters 189 (1992) 119.

[18] S. Mukamel and H.X. Wang, Phys. Rev. Letters, submitted for publication.

[19] M. Pope and C. Swenberg, Electronic processes in organic crystals (Oxford Univ. Press, Oxford, 1982).

[20] F.C. Spano and S. Mukamel, Phys. Rev. A 40 (1989) 5783;
Phys. Rev. Letters 66 (1991) 1197;
O. Dubovsky and S. Mukamel, J. Chem. Phys. 95 (1991) 7828;
S. Mukamel, in: Nonlinear optical properties of organic molecules and crystals, Vol. 3, ed. J. Zyss (Academic Press, New York), in press.

[21] B.I. Greene, J. Orenstein and S. Schmitt-Rink, Science 247 (1990) 679.

[22] O. Dubovsky and S. Mukamel, J. Chem. Phys., in press.

[23] H.F. Hameka, J. Chem. Phys. 67 (1977) 2935;
E.F. McIntyre and H.F. Hameka, J. Chem. Phys. 68 (1978) 5534.